Original Article

MOLECULAR METABOLISM

Direct small molecule ADaM-site AMPK activators reveal an AMPKγ3-independent mechanism for blood glucose lowering

Nicolas O. Jørgensen [1], Rasmus Kjøbsted [1], Magnus R. Larsen [1], Jesper B. Birk [1], Nicoline R. Andersen [1], Bina Albuquerque [2], Peter Schjerling [3,4], Russell Miller [2], David Carling [5], Christian K. Pehmøller [2], Jørgen F.P. Wojtaszewski [1,*]

ABSTRACT

Objective: Skeletal muscle is an attractive target for blood glucose-lowering pharmacological interventions. Oral dosing of small molecule direct pan-activators of AMPK that bind to the allosteric drug and metabolite (ADaM) site, lowers blood glucose through effects in skeletal muscle. The molecular mechanisms responsible for this effect are not described in detail. This study aimed to illuminate the mechanisms by which ADaM-site activators of AMPK increase glucose uptake in skeletal muscle. Further, we investigated the consequence of co-stimulating muscles with two types of AMPK activators i.e., ADaM-site binding small molecules and the prodrug AICAR.

Methods: The effect of the ADaM-site binding small molecules (PF739 and 991), AICAR or co-stimulation with PF739 or 991 and AICAR on muscle glucose uptake was investigated *ex vivo* in *m. extensor digitorum longus* (EDL) excised from muscle-specific AMPKα1α2 as well as whole-body AMPKγ3-deficient mouse models. *In vitro* complex-specific AMPK activity was measured by immunoprecipitation and molecular signaling was assessed by western blotting in muscle lysate. To investigate the transferability of these studies, we treated diet-induced obese mice *in vivo* with PF739 and measured complex-specific AMPK activation in skeletal muscle.

Results: Incubation of skeletal muscle with PF739 or 991 increased skeletal muscle glucose uptake in a dose-dependent manner. Co-incubating PF739 or 991 with a maximal dose of AICAR increased glucose uptake to a greater extent than any of the treatments alone. Neither PF739 nor 991 increased AMPKα2β2γ3 activity to the same extent as AICAR, while co-incubation led to potentiated effects on AMPKα2β2γ3 activation. In muscle from AMPKγ3 KO mice, AICAR-stimulated glucose uptake was ablated. In contrast, the effect of PF739 or 991 on glucose uptake was not different between WT and AMPKγ3 KO muscles. *In vivo* PF739 treatment lowered blood glucose levels and increased muscle AMPKγ1-complex activity 2-fold, while AMPKα2β2γ3 activity was not affected.

Conclusions: ADaM-site binding AMPK activators increase glucose uptake independently of AMPKγ3. Co-incubation with PF739 or 991 and AICAR potentiates the effects on muscle glucose uptake and AMPK activation. *In vivo*, PF739 lowers blood glucose and selectively activates muscle AMPKγ1-complexes. Collectively, this suggests that pharmacological activation of AMPKγ1-containing complexes in skeletal muscle can increase glucose uptake and can lead to blood glucose lowering.

Keywords AMP-activated protein kinase; Skeletal muscle; Glucose uptake; Metabolism; Metabolic disease

1. INTRODUCTION

AMP-activated protein kinase (AMPK) is a ubiquitously expressed and highly conserved multisubstrate serine and threonine kinase [1]. It is often referred to as an energy sensor of the cell, as cellular energy fluctuations lead to its activation [1]. AMPK is a heterotrimeric protein complex consisting of one α-, β-, and γ-subunit [2]. The α-subunit includes the kinase domain, while the β- and γ-subunits are regulatory in function. The β-subunit includes a sensory domain for glycogen, while the γ-subunit binds adenosine nucleotides that provide AMPK with the ability to sense fluctuations in glycogen content and the adenosine nucleotide pools [2]. AMPK-subunit proteins exist in various isoforms (α1/α2, β1/β2, and γ1/γ2/γ3). This enables the existence of 12 different heterotrimeric complexes, but the complex expression is both species- and tissue-specific. Three complexes exist in human skeletal muscle, whereas mouse muscle expresses five [3,4]. In addition to AMPKα1β2γ1, AMPKα2β2γ1, and AMPKα2β2γ3, which are found in human *m. vastus lateralis*, AMPKα1β1γ1 and α2β1γ1 are also found in mouse muscle e.g., *m. extensor digitorum longus* (EDL) [4]. Across species, the AMPKγ3 subunit is primarily expressed in skeletal muscle

[1]Section of Molecular Physiology, Department of Nutrition, Exercise and Sports, Faculty of Science, University of Copenhagen, Copenhagen, Denmark [2]Internal Medicine Research Unit, Pfizer Global Research and Development, Cambridge, MA, USA [3]Institute of Sports Medicine Copenhagen, Department of Orthopedic Surgery, Copenhagen University Hospital - Bispebjerg and Frederiksberg, Copenhagen, Denmark [4]Center for Healthy Aging, Institute for Clinical Medicine, University of Copenhagen, Copenhagen, Denmark [5]MRC London Institute of Medical Sciences, Imperial College London, Hammersmith Hospital, London W12 0NN, UK

*Corresponding author. Universitetsparken 13, DK-2100 Copenhagen Ø, Denmark. E-mail: jwojtaszewski@nexs.ku.dk (J.F.P. Wojtaszewski).

Received April 29, 2021 • Revision received May 13, 2021 • Accepted May 14, 2021 • Available online 23 May 2021

https://doi.org/10.1016/j.molmet.2021.101259

and only in complex with AMPKα2β2. The AMPKα2β2γ3 complex is primarily found in glycolytic skeletal muscle [4–7].

The prodrug 5-aminoimidazole-4-carboxyamide ribonucleotide (AICAR) is phosphorylated intracellularly to ZMP (an AMP-analogue). ZMP binds to the γ-subunit of AMPK causing its activation and an increase in skeletal muscle glucose uptake [8]. AICAR-induced muscle glucose uptake is AMPK-dependent and independent of proximal insulin signaling [9–11]. Furthermore, the activation of AMPK has been shown to increase skeletal muscle insulin sensitivity [12–14]. As AMPK signaling is not compromised in insulin-resistant human muscle [15], these findings suggest that skeletal muscle AMPK is a relevant target for human pharmacological glucose lowering interventions, especially in metabolic diseases such as type-2 diabetes [16,17]. One approach to activate AMPK is to introduce an AMP analogue like ZMP in the muscle cell, thus mimicking energy fluctuations. Our group and others have provided genetic evidence to support that AICAR-induced glucose uptake in skeletal muscle is dependent on AMPKα2 [10], AMPKβ2 [18], and AMPKγ3 [19]. Collectively, this suggests that AICAR-induced glucose uptake is dependent on the muscle-specific AMPKα2β2γ3 complex, and thus particularly potent in glycolytic skeletal muscle. However, because AMP (or ZMP) regulates several cellular processes and the bioavailability of AICAR is low when orally ingested [20], AICAR is not an attractive drug for human pharmacological interventions.

Structural studies of AMPK have identified the allosteric drug and metabolite-site (ADaM-site) [21]. This highly conserved pocket between the AMPKα- and β-subunits was described as a potential binding site for endogenous AMPK-regulating metabolite(s). One of these metabolites was recently discovered [22]. Importantly, the identification of the ADaM-site led to the discovery of a new class of pharmacological compounds that directly target the ADaM-site and activate AMPK [16,17,21,23–26]. The ADaM-site binding small molecule pan-activators of AMPK (991, PF739, MK-8722, and SC4) increase glucose uptake into skeletal muscle [16,17,24–26]. Importantly, both PF739 and MK-8722 are capable of lowering blood glucose levels in diabetic rodent models and nonhuman primates [16,17], an effect dependent on skeletal muscle AMPK [16]. As these compounds are pan-activators of AMPK, they are expected to activate AMPK in all cells of the body. Therefore, undesired effects of *in vivo* treatment have been described e.g., cardiac hypertrophy and glycogen buildup in cardiac muscle [17]. The mechanisms by which ADaM-site-binding AMPK activators increase skeletal muscle glucose uptake are still only rudimentarily understood. We anticipate that insight into these mechanisms will illuminate a road toward the development of AMPK-targeting drugs that specifically activate skeletal muscle AMPK; an approach, which seems viable for glucose lowering interventions in human metabolic diseases.

The study was aimed to illuminate the mechanisms by which the ADaM-site activators of AMPK increase glucose uptake in skeletal muscle. We hypothesized that ADaM-site binding AMPK activators would increase glucose uptake through the same mechanism as AICAR i.e., through the AMPKα2β2γ3 complex. Further, we hypothesized that AICAR in combination with the ADaM-site-binding AMPK activators would potentiate the stimulation of AMPK activity.

2. METHODS

2.1. Animals

All mice had free access to standard rodent chow and drinking water, and were maintained on a 12:12 h light–dark cycle in a temperature-controlled room (20–22 °C). All mice used were females aged 12–25 weeks. All experiments were approved by the Danish Animal Experiments Inspectorate (License #2014-15-2934-01037 and #2019-15-0201-01659) and complied with the European Union guidelines for the protection of vertebra animals used for scientific purposes.

PRKAG3 KO (from here on AMPKγ3 KO) mice were generated by the CRISPR-Cas9 method at Jackson Laboratories (Bar Harbor, ME, USA) in the C57BL/6J background strain using the Prkag3exon6 sgRNA (CATGGTGGCCAACGGTGTGA). Founder animals were screened by PCR amplification and sequencing to confirm a frameshift deletion resulting in a premature stop codon (Figure S1A-B). Founder animals were bred with C57BL/6J mice for >8 generations before reported experiments. The experimental cohorts were bred as homozygotes and represented the F1 and F2 generations. The genotype of all wild-type (WT) and AMPKγ3 KO mice were determined from the DNA of ear clips using qPCR with primers for WT (CCATGGTGGCCAACGGTGTG and GAGGTCCAGCCACCTCTCCTCA) and KO (CCATGGTGGCCAACAGCTCC and CACCCACAAAGCTCTGCTTCTTGCT) in parallel reactions.

In this study, the constitutive muscle-specific AMPKα1α2 double knockout mouse model (AMPKα1α2 mdKO) [27,28] and the inducible muscle-specific AMPKα1α2 double knockout mouse model (AMPKα1α2 imdKO) [11] were also used. Tamoxifen was injected thrice within one week to initiate gene deletion. The animals were injected three weeks before the experiments [11]. The WT mice corresponding to the AMPKα1α2 mdKO and imdKO are double-floxed for AMPKα1 and AMPKα2, but lack the Cre expression. WT mice for imdKO were also treated with tamoxifen.

2.2. Ex vivo compound-stimulated glucose uptake in mouse muscle

Fed mice were anesthetized by an intraperitoneal injection of a mix of pentobarbital (100 mg/kg body weight) and xylocaine (5.0 mg/kg body weight) before both *m. soleus* (Sol) and/or *m. extensor digitorum longus* (EDL) muscles were excised from the hindlimbs. The muscles were suspended at resting tension (≈0.5 mN) in incubation chambers (Danish MyoTechnology, Denmark). Before muscle incubation, the chambers were filled with preheated (30 °C) Krebs–Ringer buffer (117 mM NaCl, 4.7 mM KCl, 2.5 mM $CaCl_2$, 1.2 mM KH_2PO_4, 1.2 mM $MgSO_4$, 24.6 mM $NaHCO_3$, pH = 7.4) supplemented with 0.1% bovine serum albumin, 2 mM Na-pyruvate, and 8 mM mannitol. Throughout the entire incubation protocol, the buffer was gassed with 95% O_2 and 5% CO_2. The muscles were allowed to recover from dissection for 10 min in the incubation chambers before the buffer medium was replaced and stimulation was initiated. Muscles were stimulated with DMSO-dissolved PF739 and 991 for 40 and 60 min, respectively. Within a given experiment, the DMSO concentration used was equal between treatments and always less than 0.08%. During the last 10 min of stimulation, 1 mM [^{3}H]-2-deoxyglucose (0.028 MBq/mL) and 7 mM [^{14}C]mannitol (0.0083 MBq/mL) were added to the incubation medium. After incubation, the muscles were harvested, washed in cold (4 °C) Krebs–Ringer buffer, blotted dry on filter paper, and frozen in liquid nitrogen. Glucose uptake was determined from muscle lysate as previously described [13].

2.3. In vivo treatment of PF739 of diet-induced obese mice

PF739 was suspended in 20% (2-hydroxypropyl)-β-cyclodextrin (HPBCD) as a solution in isotonic saline (20 mg/mL). The mice were 15 weeks old C57BL/6J mice and had been fed a diet of 60% fat, 20% carbohydrates, and 20% protein (D12492, Research Diets Inc.) for 9 weeks before the experiment. The mice were dosed subcutaneously with 100 mg/kg bodyweight of PF739 or vehicle. One hour after treatment, the mice were anesthetized with isoflurane-O_2 and muscle

tissues were harvested and frozen in liquid nitrogen immediately, using cooled metal clamps. Glucose levels were determined in tail blood before and 1 h after treatment of the animals.

2.4. Muscle homogenization

Muscles, cold steel beads, and cold (4 °C) homogenization buffer (10% glycerol, 50 mM HEPES, 1% NP40, 20 mM $Na_4P_2O_7$, 150 mM NaCl, 2 mM PMSF, 1 mM EDTA, 1 mM EGTA, 3 mM benzamidine, 10 μg/mL leupeptin, 10 μg/mL aprotinin, 2 mM Na_3VO_4, pH = 7.5) were added to Eppendorf tubes. The muscles were homogenized at 30 Hz for 2 × 45 s (TissueLyser II, Qiagen, Germany) and were subsequently rotated end-over-end for 1 h at 4 °C. Next, the homogenates were spun for 20 min at 16.000 g and 4 °C, and the lysates (supernatant) were collected and frozen at −80 °C until further analyses. Protein concentration in the lysates was determined using the bicinchoninic acid method as described by the manufacturer (Pierce Biotechnology, Thermo Fisher, MA, USA).

2.5. SDS-PAGE and western blotting

Lysate from muscle samples were denatured in Laemmli buffer (final concentrations: 1.8% SDS, 56.7 mM tris (pH = 6.8), 37.5 mM DTT, 3.3% glycerol, and 0.008% bromphenol blue) and heated at 96 °C for 5 min. Equal amounts of protein were loaded on 5–7% polyacrylamide gels for separation. The proteins separated in the gel were transferred to ethanol-activated polyvinylidene fluoride membranes, by semidry western blotting. The membranes were blocked in TBST (10 mM tris, 150 mM NaCl, and 0.05% Tween20, pH = 7.4) supplemented with 2% skimmed milk powder except for membranes used to detect ACC total, for which 3% bovine serum albumin was used. Thereafter, the membranes were incubated with specific primary total- or phospho-antibodies overnight on a rocking table at 4 °C. The probed membranes were washed in TBST before incubation with relevant secondary antibodies for 45 min at room temperature on a rocking table. Following yet another wash in TBST, the membranes were visualized by chemiluminescence and a digital imaging system (ChemiDoc XRS+, BioRad, USA).

2.6. Complex-specific AMPK activity

Complex-specific AMPK activity was measured as previously described [29]. Muscle lysate (150 μg protein) underwent sequential immunoprecipitations of first AMPKγ3, then AMPKα2, and lastly AMPKα1 using in-house validated AMPK subunit-specific antibodies bound to G-protein coupled agarose beads (Merck, Darmstadt, Germany) in an IP-buffer (20 mM tris (pH = 7.4), 50 mM NaCl, 1% (v/v) Triton X-100, 50 mM NaF, 5 mM $Na_4P_2O_7$, 500 μM PMSF, 2 mM DTT, 4 μg/mL leupeptin, 50 μg/mL soybean trypsin inhibitor, 6 mM benzamidine, 250 mM sucrose). The first immunoprecipitation was rotated end-over-end at 4 °C overnight, where after the beads were spun down (1 min at 500 g, 4 °C) and the supernatant was removed and used for the next immunoprecipitations. The beads were washed once in the IP-buffer, once in cold 6x assay buffer (240 mM HEPES (pH = 7.0), 480 mM NaCl) and twice in cold 3x assay buffer (120 mM HEPES (pH = 7.0), 240 mM NaCl), where after the supernatant was removed leaving only the beads. The activity assays were performed for 30 min at 30 °C in a kinase reaction buffer (40 mM HEPES (pH = 7.0), 80 mM NaCl, 833 μM DTT, 100 μM AMARA-peptide, 5 mM $MgCl_2$, 200 μM ATP) including 60 μCi/mL [$^{33}P_\gamma$]-labelled ATP tracer (Perkin Elmer, Waltham, USA). The kinase reaction was stopped by the addition of 1% phosphoric acid to the reaction. The reactions were spotted on P81 filter paper and excess phosphate tracer was washed off the paper by incubation with 1% phosphoric acid for 3 × 15 min. The [^{33}P] activity was analyzed on dry filter paper, using a Typhoon FLA 700 IP PhosphorImager (GE Healthcare, Denmark), and related to the specific activity of the reaction buffer that was measured using liquid scintillation counting. This process was repeated for the α2- and α1-immunoprecipitation to provide activity measurements for the remaining AMPK complexes. In the present study, the AMPKγ3 activity and the remnant activity that can be precipitated by subsequent precipitations using AMPKα2 and -α1 antibodies are reported. The latter activities are presented as the sum of the two AMPKα precipitations, and for simplicity, we termed this as AMPKγ1 activity since skeletal muscle does not contain AMPKγ2 [4].

2.7. Insulin and glucose tolerance tests

Before testing, 12–13-week-old mice were weighed and placed in individual cages with access to drinking water, but not food. The mice were subjected to fasting for 4 or 16 h before the insulin (ITT) and glucose tolerance test (GTT), respectively. For the ITT, the mice were injected i.p. with 0.75 U/kg body weight of insulin (Actrapid, Novo Nordisk, Denmark) dissolved in physiological saline (0.9%) and blood samples were obtained from the tail before injection and 15, 30, 60, and 120 min into the ITT. For the GTT, the mice were injected i.p. with 2 g/kg bodyweight of D-glucose dissolved in physiological saline (20% glucose solution). Blood samples were obtained from the tail before and 15, 30, 60, and 120 min following the glucose injection. Blood glucose concentrations were determined by using a glucometer (Contour XT, Bayer, Germany).

2.8. Primary and secondary antibodies

Primary antibodies used for western blotting were as follows: Phospho-specific antibodies recognizing pAMPKα Thr172 (#2531) and pACC Ser212 (#3661) were from Cell Signaling Technology (Danvers, MA, USA); phospho-specific antibody recognizing pTBC1D1 Ser231 was from Millipore (#07–2269); total AMPKα1 was custom and a gift from Prof. Göransson (Lund University, Sweden); AMPKα2, and AMPKβ1 were from Santa Cruz Biotechnology (#SC-19131 and #SC-100357, Santa Cruz, CA, USA); AMPKβ2 was custom and a gift from Prof. Hardie (Dundee University, UK); AMPKγ1 and TBC1D1 were from Abcam (#32508 and #ab229504, Cambridge, UK); and AMPKγ3 was custom made at Yenzym (YZ-6229, San Francisco, CA, USA). Total ACC was measured using HRP-conjungated streptavidin from either DAKO (#P0397, Glostrup, Denmark) or Jackson ImmunoResearch Laboratories (#108001, West Grove, PA, USA).

Secondary antibodies used in this study were all horseradish peroxidase-conjugated species-specific immunoglobulins and included antirabbit (#111-035-045), antimouse (#115-035-062), and antigoat (#305-035-003) from Jackson ImmunoResearch Laboratories.

Antibodies used for immunoprecipitations (IP) as a part of the AMPK activity assay were as follows: AMPKα1 was precipitated with a custom antibody from Genscript (Genscript 2015, ID# 03302_1, New Jersey, USA), and AMPKα2 (YZ-7205) and AMPKγ3 (YZ-6229) were precipitated with custom antibodies from Yenzym (San Francisco, CA; USA).

2.9. Statistical analyses

Data are presented as means + SEM, unless stated otherwise. Differences between doses, treatments, or genotypes were analyzed either using unpaired two-tailed student t-tests or one-way or two-way ANOVA with or without repeated measures when relevant. The specific use of statistical tests is explicitly described in the figure legends. The Student–Newman–Keuls test was used for post hoc testing with $p < 0.05$ as the significance level. Statistical analyses were carried out using the software GraphPad Prism (version 9.1, San Diego, CA, USA).

3. RESULTS

3.1. Knockout of AMPKγ3 by CRISPR-Cas9 induces changes in protein expression of other AMPK subunits and ablates AMPKα2β2γ3 activity

To investigate the involvement of AMPKγ3 in mechanisms relevant for pharmacological regulation of glucose uptake, AMPKγ3 KO mice were generated by the CRISPR-Cas9 technique (Figure S1A-B). The AMPKγ3 KO mice were equal in size when compared with their WT counterparts (data not shown). AMPKγ3 protein was detected in glycolytic skeletal muscle such as *m. extensor digitorum longus* (EDL), *m. gastrocnemius* (Gast), *m. tibialis anterior* (TA), and *m. quadriceps* (Quad), but very low or undetectable in oxidative muscle *m. soleus (Sol)*, heart muscle, or liver (Figure 1A + I). As expected, AMPKγ3 protein expression was ablated in the muscles of the AMPKγ3 KO mice (Figure 1A + I). The expression of AMPKα2 and -β2 protein, which assemble in a protein complex with AMPKγ3, was significantly lower in Gast, TA, and Quad muscles of the AMPKγ3 KO compared to WT mice (Figure 1B, C + I). AMPKα1, -β1, and -γ1 protein were detected in all tissues with no or minor differences between genotypes (Figure 1D—F + I). Basal AMPKα2β2γ3 activity was not detectable in muscles from AMPKγ3 KO mice (EDL, Sol, and TA, Figure 1G). There were no significant differences in basal AMPKγ1 complex activity between genotypes (Figure 1H).

Fasted WT and AMPKγ3 KO mice were subjected to insulin and glucose tolerance tests (Figure 1J—K). Fasted blood glucose levels were unaffected by the AMPKγ3 deficiency and the blood glucose lowering effect of insulin was similar between genotypes (Figure 1J). The response to a glucose tolerance test was also comparable between genotypes (Figure 1K).

3.2. PF739 and AICAR co-stimulation potentiates the effect on glucose uptake and AMPK activity

The *ex vivo* dose—response relationship between increasing doses of PF739 and glucose uptake was investigated in EDL (Figure 2A) and Sol (Figure 2B) muscle excised from C57BL/6J mice. Glucose uptake in EDL muscle increased in a dose-dependent manner, while glucose uptake in Sol remained unaffected, even when the dose of PF739 was 10-fold higher than that used for EDL. Similarly, stimulation of the muscles with a maximal dose of AICAR (2 mM) [13] increased glucose uptake in EDL, but not in Sol (Figure 2A—B).

In a separate experiment, glucose uptake was investigated in EDL muscles stimulated *ex vivo* with either maximal PF739 (3 μM), maximal AICAR (2 mM), or co-incubated with PF739 (3 μM) and AICAR (2 mM) (Figure 2C). PF739 and AICAR treatment increased glucose uptake 2-fold, but surprisingly, the combination of the two AMPK activators potentiated the effect on glucose uptake. PF739 treatment did not induce any significant activation of AMPKα2β2γ3, while AICAR led to a 3-fold increase. The co-stimulation with PF739 and AICAR activated AMPKα2β2γ3 to even higher levels compared to AICAR alone (more than 6-fold) (Figure 2D) indicated potentiating effects when the two compounds were combined.

3.3. The potentiating effect of PF739 and AICAR co-stimulation on muscle glucose uptake is dependent on AMPK catalytic activity

We investigated whether the potentiating effect of PF739 and AICAR co-stimulation on glucose uptake was dependent on AMPK catalytic activity by introducing the AMPKα1α2 imdKO mouse model that lacks all AMPKα protein expression and activity in skeletal muscle cells [11]. EDL muscles were stimulated with PF739 (3 μM), AICAR (2 mM), or a combination of the two compounds. While glucose uptake in vehicle-treated muscle was equivalent between WT and AMPKα1α2 imdKO mice, the increase in glucose uptake observed in WT muscle stimulated with PF739, AICAR, and the combination of PF739 and AICAR was completely absent in the muscle from the AMPKα1α2 imdKO mice (Figure 3A). In WT muscle, AMPKα2β2γ3 activity was not increased significantly by PF739 treatment, though AICAR stimulation led to a substantial activation (Figure 3B). Also, in this experiment, co-incubation with PF739 and AICAR led to an even greater increase in AMPKα2β2γ3 activity compared to the isolated effect of AICAR, suggesting potentiating effects of the co-stimulation. As expected, AMPKα2β2γ3 activity was not detected in the muscle from AMPKα1α2 imdKO mice by any of the treatments (Figure 3B). In WT muscle, AMPK Thr172 phosphorylation followed the pattern of the AMPKα2β2γ3 activity (Figure 3C + F). Phosphorylation of the AMPK downstream target ACC Ser212 (Figure 3D + F) was increased by PF739, and to a greater extent by AICAR and the co-incubation. Phosphorylation of TBC1D1 Ser231 (Figure 3E—F) was increased to similar levels among treatments. The increases observed in phosphorylation of ACC Ser212 and TBC1D1 Ser231 in muscle from AMPKα1α2 imdKO mice are likely due to the activation of AMPKα1 complexes present in nonmuscle cells (Figure 3D—F, S2A) [11]. In line, AMPKα1 protein was detected during analysis of the muscle protein lysate from the AMPKα1α2 imdKO mice, while AMPKα2 protein was not detectable (Figure S2A).

3.4. AMPKγ3 is not necessary for PF739-stimulated glucose uptake

We used the AMPKγ3 KO model to investigate the AMPK-dependent mechanism by which PF739 increases glucose uptake. Furthermore, it was investigated if the potentiating effects observed by PF739 and AICAR co-incubation were caused by AMPKγ3-dependent regulation. In EDL muscle from WT mice, glucose uptake increased in response to *ex vivo* PF739 and AICAR stimulation (Figure 4A) in a similar pattern as observed in the previous experiments (Figures 2C and 3A). Surprisingly, PF739-stimulated glucose uptake was intact in muscle from AMPKγ3 KO mice, while AICAR stimulation did not affect glucose uptake. Even though AICAR did not increase glucose uptake in AMPKγ3 KO muscle, the co-stimulation with PF739 and AICAR still increased glucose uptake to a greater extent than that of PF739 alone, suggesting that AICAR still potentiates the effect of PF739 on glucose uptake (Figure 4A). Here, PF739 increased the AMPKα2β2γ3 activity to a small extent, whereas AICAR and the co-incubation activated the complex 5- and 10-fold, respectively, exceeding the PF739 effect substantially (Figure 4B). AMPKα2β2γ3 activation was not detected in muscle from AMPKγ3 KO mice (Figure 4B). The AMPKγ1-complex activity was increased significantly only by the co-incubation in WT muscle, while it was also activated by AICAR and the co-incubation in AMPKγ3 KO muscle (Figure 4C). AMPK Thr172 phosphorylation was increased by PF739 in WT muscle. AICAR stimulation induced an even higher degree of phosphorylation, whereas the co-incubation led to the most potent phosphorylation of AMPK Thr172 (Figure 4D + G). In AMPKγ3 KO muscle, PF739 stimulation did not increase the AMPK Thr172 phosphorylation levels significantly, but AICAR did. Further, the co-incubation

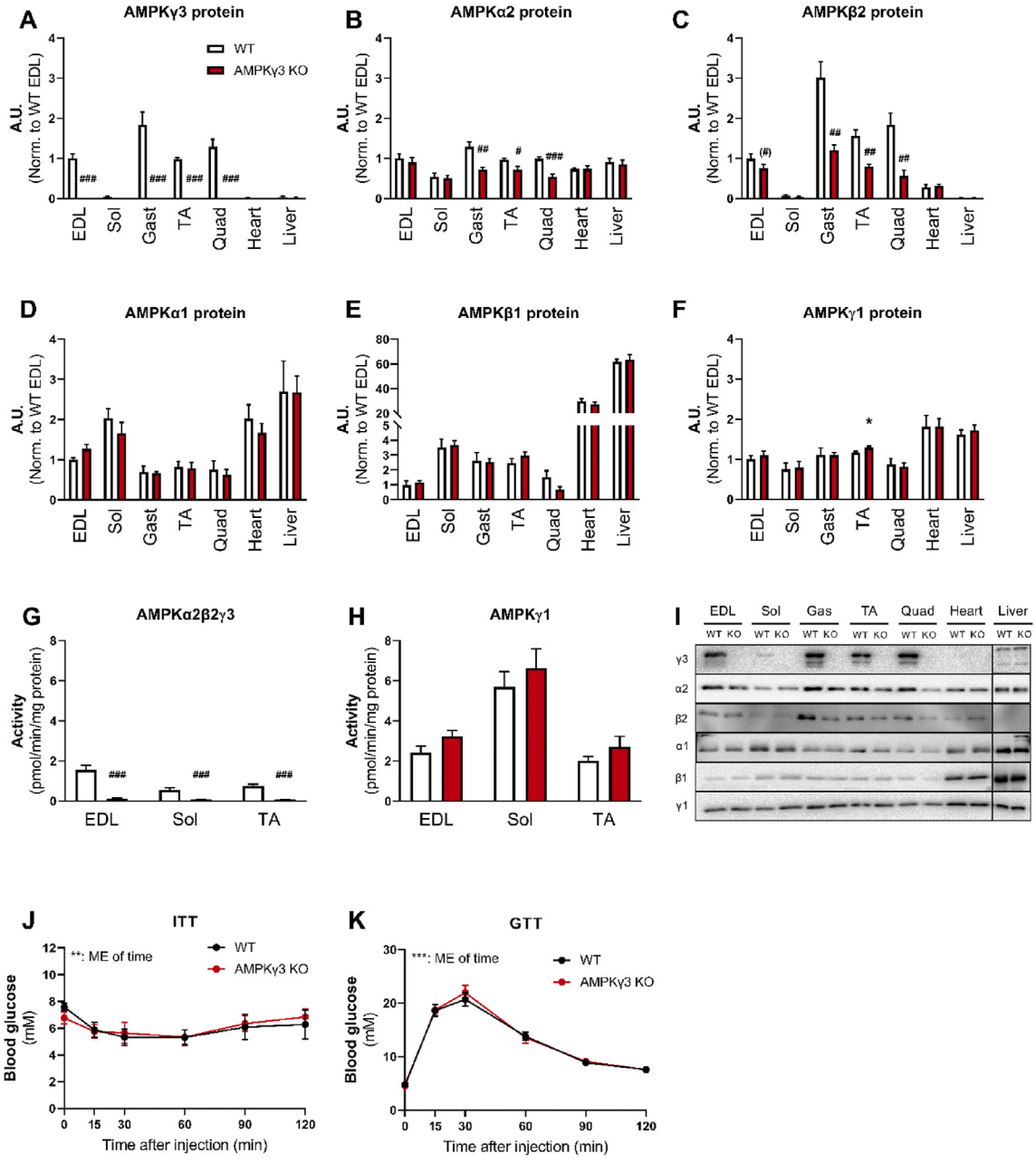

Figure 1: *CRISPR-Cas9 guided deletion of AMPKγ3 protein in adult mice.* The CRISPR-Cas9 system was used for specific deletion of AMPKγ3 protein expression in mice. A–F: Protein expression levels of (A) AMPKγ3, (B) AMPKα2, (C) AMPKβ2, (D) AMPKα1, (E) AMPKβ1, and (F) AMPKγ1 in extensor digitorum longus (EDL), soleus (Sol), gastrocnemius (Gast), tibialis anterior (TA) and quadriceps (Quad) muscle along with heart muscle, and liver from adult female WT and AMPKγ3 KO mice. Protein levels were measured by western blotting. Data are normalized to WT EDL levels. Data are given as means + SEM (n = 5 in all groups). G–H: *In vitro* complex-specific AMPK activity of G) AMPKα2β2γ3-and (H) AMPKγ1-complex activity was measured in EDL, Sol, and TA from basal WT and AMPKγ3 KO mice. The AMPK activity was measured after sequential immunoprecipitation from muscle lysates in the order AMPKγ3, AMPKα2, and AMPKα1. The latter two are added together for simplicity. Data are given as means + SEM (n = 8 in EDL and Sol, n = 12 in TA). I: Representative blots of the proteins measured in A-F. Liver measurements were performed on the same membrane as skeletal and heart muscle. WT and AMPKγ3 KO are indicated with white and red bars, respectively. An unpaired students t-test was applied to compare WT and AMPKγ3 KO within each muscle. *p < 0.05, #p < 0.05, ##p < 0.01, and ###p < 0.001 for differences in AMPKγ3 KO compared to WT. J–K: (J) Intraperitoneal insulin tolerance test (ITT, 0.75 U/kg body weight) and (K) intraperitoneal glucose tolerance test (GTT, 2 mg/kg body weight) were performed in WT and AMPKγ3 KO mice. Data are given as means +/− SEM (n = 4–9). WT and AMPKγ3 KO mice are indicated with black and red dots and lines, respectively. A two-way RM ANOVA was used to compare WT and AMPKγ3 KO mice. **p < 0.01, ***p < 0.001 indicates main effects of time. A.U., Arbitrary Units. . (For interpretation of the references to colour in this figure legend, the reader is referred to the Web version of this article.)

led to even higher levels of AMPK Thr172 phosphorylation, compared to AICAR alone (Figure 4D + G). Phosphorylation of ACC Ser212 increased in muscle from both WT and AMPKγ3 KO mice in response to all treatments, though the co-stimulation increased the phosphorylation to a greater extent compared to the isolated effects of PF739 and AICAR (Figure 4E + G). In WT muscle, AICAR and co-incubation increased the

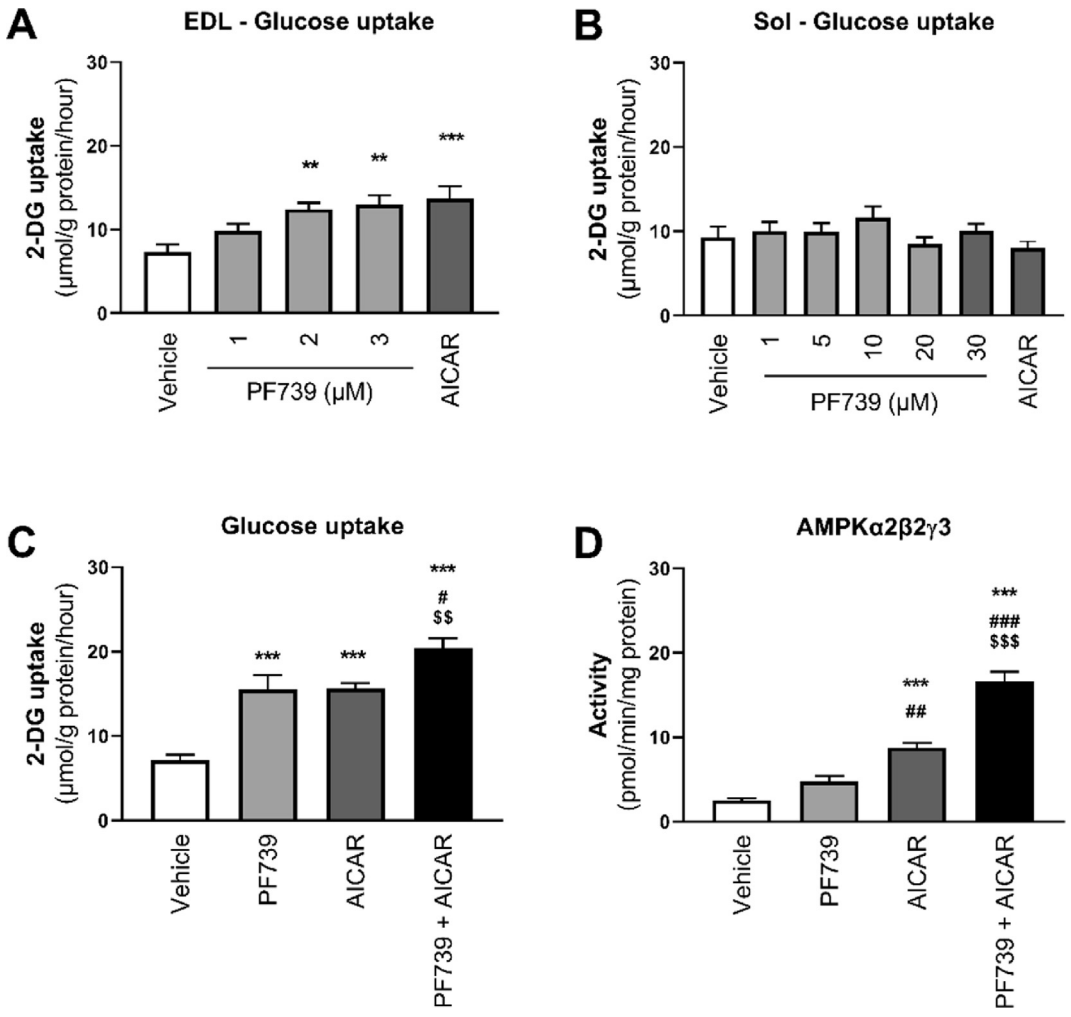

Figure 2: *Co-stimulation with PF739 and AICAR causes potentiation of glucose uptake in skeletal muscle.* A—B: *M. extensor digitorum longus* (EDL) and *m. soleus* (Sol) were dissected from C57BL/6J mice and incubated *ex vivo* for 40 min with varying doses of PF739 with vehicle (DMSO) and AICAR (2 mM) as negative and positive controls, respectively. Muscle glucose uptake was determined in (A) EDL and (B) Sol muscles by measuring the intracellular accumulation of [^{3}H]-2-deoxyglucose-6-phosphate during the last 10 min of compound stimulation ($n = 6-12$). C—D: EDL muscles were dissected from C57BL/6J mice and incubated *ex vivo* for 40 min with either vehicle (DMSO), PF739 (3 µM), AICAR (2 mM), or a combination of PF739 (3 µM) and AICAR (2 mM). (C) Muscle glucose uptake was determined as described above. (D) *In vitro* complex-specific AMPK-activity of AMPKα2β2γ3 was measured after immunoprecipitation of AMPKγ3 in muscle lysates ($n = 8-12$). Data are given as means + SEM. Vehicle, PF739, AICAR, and PF739 + AICAR treatment are indicated with white, light grey, dark grey, and black bars, respectively. An unpaired one-way ANOVA was used to compare treatment groups with vehicle (A—B) and between all groups (C—D). *$p < 0.05$, **$p < 0.01$, ***$p < 0.001$ for differences compared to vehicle, #$p < 0.05$, ##$p < 0.01$, ###$p < 0.001$ for differences compared to PF739, $$$p < 0.01$, $$$$p < 0.001$ for differences compared to AICAR alone. A.U., Arbitrary Units.

phosphorylation of TBC1D1 Ser231. In contrast, in the AMPKγ3 KO muscle, PF739 and the co-stimulation increased the phosphorylation of TBC1D1 Ser231 significantly (Figure 4F—G).

3.5. The effect of 991 on glucose uptake is dependent on AMPKα, independent of AMPKγ3, and potentiates the effect of AICAR

To confirm that the difference in mechanism and the potentiation of AICAR and PF739 are caused by different modes of binding to AMPK, we compared the effect of AICAR with 991 that also activates AMPK via the ADaM-site.

The dose—response relationship between increasing doses of 991 on glucose uptake was investigated *ex vivo* in EDL muscle from C57BL/6J mice. 991 increased muscle glucose uptake in a dose-dependent manner and to levels comparable to that of a maximal concentration of AICAR (Figure 5A). The effect of 991 stimulation on glucose uptake was dependent on AMPKα as no increase in glucose uptake was observed in muscle from AMPKα1α2 mdKO mice (Figure 5B, S5A).

We isolated and treated EDL muscles from WT and AMPKγ3 KO mice with a high 991 dose (40 µM), maximal AICAR dose (2 mM), or co-incubated with 991 (40 µM) and AICAR (2 mM). We did this, firstly, to investigate whether 991 and AICAR co-stimulation potentiates the regulation of glucose uptake, and secondly, to investigate if the effect of 991 on glucose uptake is AMPKγ3-dependent. Interestingly, 991 and AICAR increased glucose uptake approximately 3-fold, while the co-stimulation increased glucose uptake even more (Figure 5C). Additionally, the increase in glucose uptake stimulated by 991 was not dependent on AMPKγ3, as glucose uptake was increased to

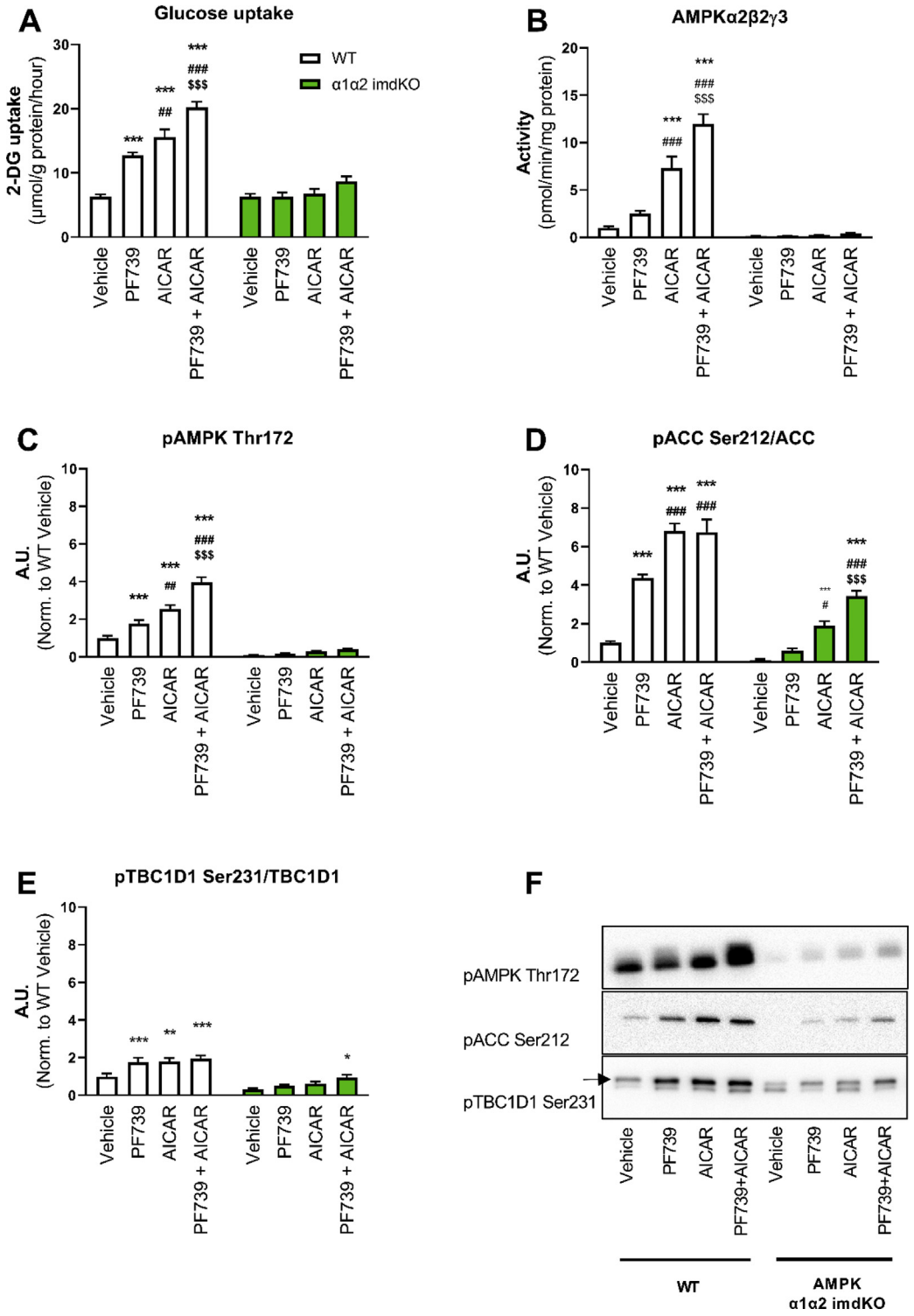

Figure 3: *The potentiating effect of PF739 and AICAR co-stimulation on glucose uptake in skeletal muscle is dependent on AMPK catalytic activity.* A–F: *M. extensor digitorum longus* (EDL) was dissected from WT and AMPKα1α2 imdKO mice and incubated *ex vivo* for 40 min with either vehicle, PF739 (3 μM), AICAR (2 mM), or a combination of PF739 (3 μM) and AICAR (2 mM). (A) Muscle glucose uptake was determined by measuring the intracellular accumulation of [^{3}H]-2-deoxyglucose-6-phosphate during the last 10 min of compound stimulation. (B) *In vitro* complex-specific AMPK-activity of AMPKα2β2γ3 was measured in WT and AMPKα1α2 imdKO mice in all treatment conditions. The AMPK activity was measured after immunoprecipitation of AMPKγ3 from muscle lysates ($n = 8$). Phosphorylation levels of (C) AMPK Thr172, (D) ACC Ser212, and (E) TBC1D1 Ser231 were measured in lysates by western blotting ($n = 8$). (F) Representative blots of the proteins measured in C-E, total proteins are given in Figure S2A. Data are given as means + SEM. WT and AMPKα1α2 imdKO mice are indicated with white and green bars, respectively. A two-way ANOVA was used to compare treatment groups within genotype. *$p < 0.05$, **$p < 0.01$, ***$p < 0.001$ for difference compared to vehicle, ##$p < 0.01$, ###$p < 0.001$ for difference compared to PF739 and $$$$p < 0.001$ for difference compared to AICAR treatment. A.U., Arbitrary Units. . (For interpretation of the references to colour in this figure legend, the reader is referred to the Web version of this article.)

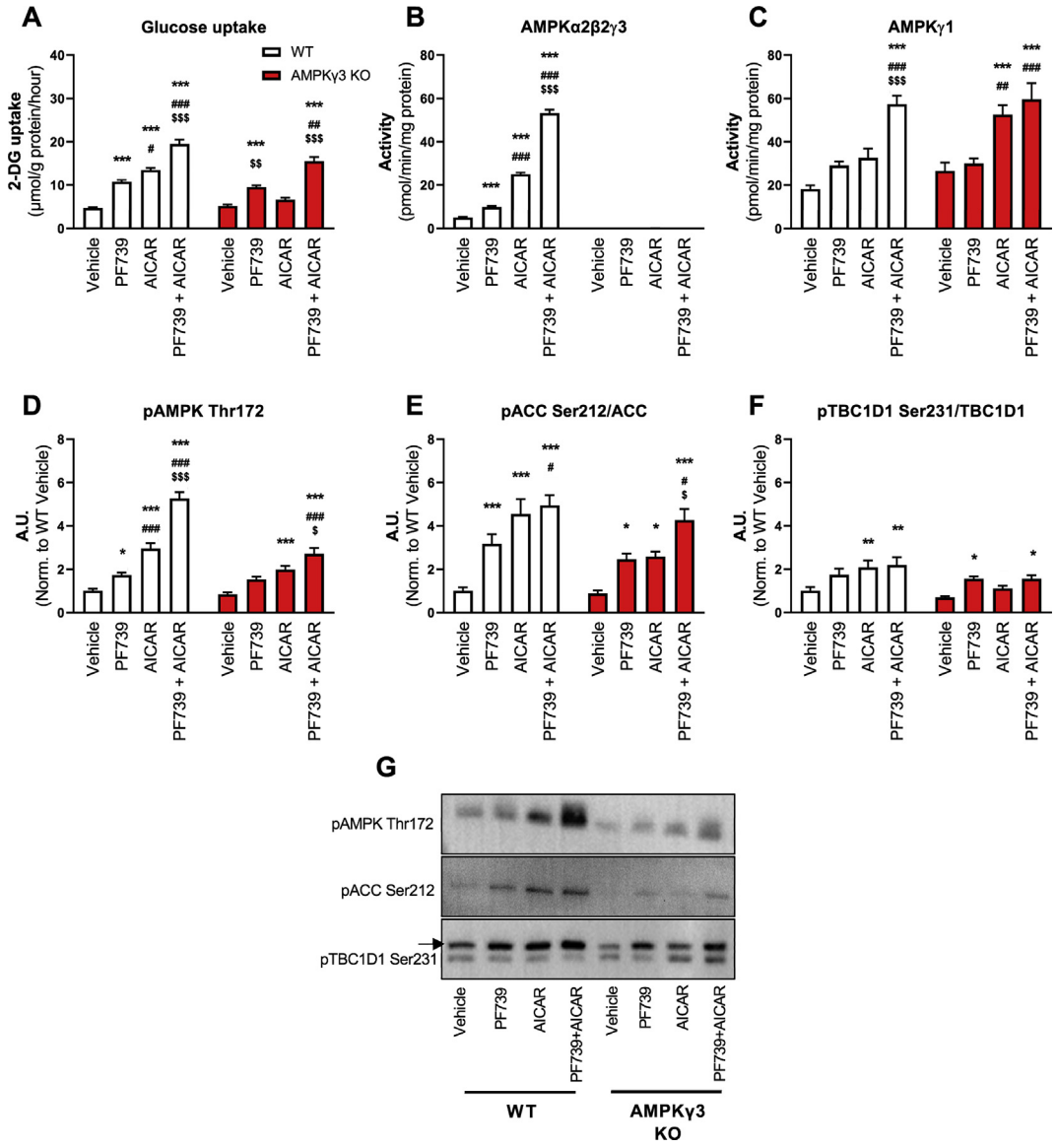

Figure 4: *In contrast to AICAR, the effect of PF739 on glucose uptake in skeletal muscle is not dependent on AMPKγ3.* A–G: *M. extensor digitorum longus* (EDL) was dissected from WT and AMPKγ3 KO mice and incubated *ex vivo* with either vehicle, PF739 (3 μM), AICAR (2 mM), or a combination of PF739 (3 μM) and AICAR (2 mM) for 40 min. (A) Muscle glucose uptake was determined by measuring the intracellular accumulation of ^{3}[H]-2-deoxyglucose-6-phosphate during the last 10 min of compound stimulation (n = 10). *In vitro* complex-specific AMPK-activity of (B) AMPKα2β2γ3 and (C) AMPKγ1 was measured in WT and AMPKγ3 KO mice in all treatment conditions. The AMPK activity was measured after sequential immunoprecipitation from muscle lysates in the order AMPKγ3, AMPKα2, and AMPKα1. The latter two are added together for simplicity (n = 10). (D) Phosphorylation levels of AMPK Thr172, (E) ACC Ser212, and (F) TBC1D1 Ser231 were measured in lysates by western blotting (n = 10). (G) Representative blots of the proteins measured in D-G, total proteins are given in Figure S3A. Data are given as means + SEM. WT and AMPKγ3 KO are indicated with white and red bars, respectively. A two-way ANOVA was used to compare treatment groups within genotype. *p < 0.05, **p < 0.01, ***p < 0.001 for differences compared to vehicle, #p < 0.05, ##p < 0.01, ###p < 0.001 for differences compared to PF739, $p < 0.05 $$p < 0.01 and $$$p < 0.001 for differences compared to AICAR treatment. A.U., Arbitrary Units. . (For interpretation of the references to colour in this figure legend, the reader is referred to the Web version of this article.)

comparable levels between genotypes. Importantly, the potentiating effect of co-incubation with 991 and AICAR was present both in WT and AMPKγ3 KO muscles (Figure 5C). AMPKα2β2γ3 activation was increased significantly by 991, and to a larger extent by AICAR stimulation, while the co-incubation led to a potentiated activation of the AMPKα2β2γ3 complex (Figure 5D). AMPKγ1-complex activity was only increased significantly by co-incubation of 991 and AICAR, but neither of the compounds alone led to any significant activation. The increase in activities was comparable between genotypes (Figure 5E). The phosphorylation of AMPK Thr172 was increased with 991, AICAR, and to a larger extent with co-incubation in WT muscle (Figure 5F + I). This potentiation was also found in the AMPKγ3 KO muscle (Figure 5F + I). In WT muscle, AICAR increased the phosphorylation of ACC Ser212 to a greater extent than 991, but this increase was not augmented further by the addition of 991 (Figure 5G + I). In the muscle from AMPKγ3 KO, the increase in phosphorylation of ACC Ser212 was equal in all intervention groups as compared to the vehicle level. The phosphorylation of TBC1D1 Ser231 was not increased significantly in

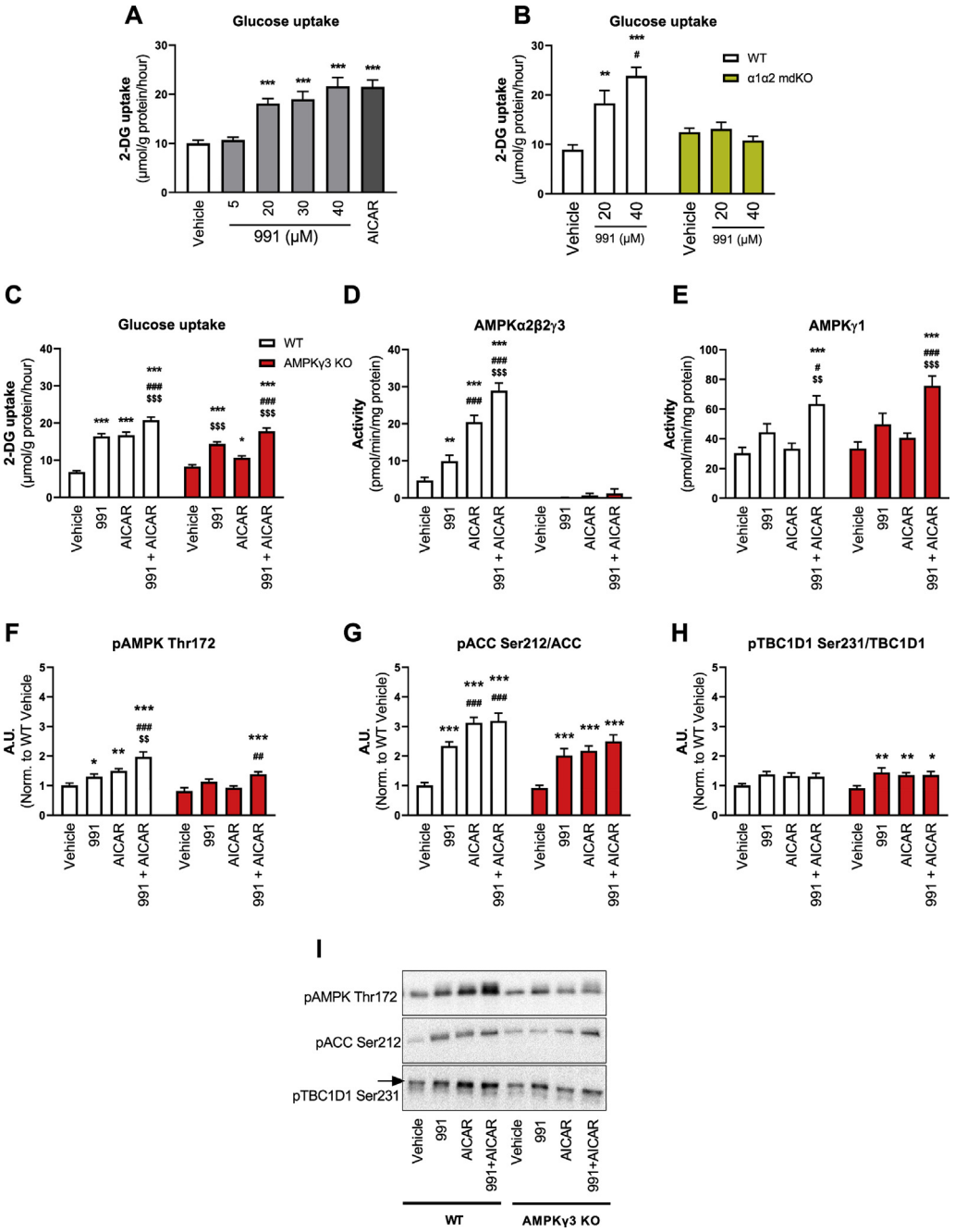

Figure 5: *The effect of ADaM-site activator 991 on glucose uptake is also AMPKα- but not AMPKγ3-dependent.* A: *M. extensor digitorum longus* (EDL) was dissected from C57BL/6J mice and incubated *ex vivo* for 60 min with varying doses of 991 with vehicle (DMSO) and AICAR (2 mM) as negative and positive controls, respectively. Muscle glucose uptake was determined by measuring the intracellular accumulation of [^{3}H]-2-deoxyglucose-6-phosphate during the last 10 min of compound stimulation (n = 4–6). Vehicle, 991, and AICAR treatments are indicated with white, light grey, and dark grey bars, respectively. B: EDL muscles were dissected from WT and AMPKα1α2 mdKO and incubated *ex vivo* for 60 min with either 20 or 40 µM 991 with vehicle (DMSO) as negative control (n = 3–6). Muscle glucose uptake was determined as described above. WT and AMPKα1α2 mdKO are indicated with white and yellow bars, respectively. C–I: EDL muscles were dissected from WT and AMPKγ3 KO mice and incubated *ex vivo* for 60 min with either vehicle (DMSO), 991 (40 µM), AICAR (2 mM), or a combination of 991 (40 µM) and AICAR (2 mM) (n = 10–12). (C) Muscle glucose uptake was determined as described above. *In vitro* complex-specific AMPK-activity of (D) AMPKα2β2γ3 and (E) AMPKγ1 was measured in WT and AMPKγ3 KO mice in all treatment conditions. The AMPK activity was measured after sequential immunoprecipitation from muscle lysates in the order AMPKγ3, AMPKα2, and AMPKα1. The latter two are added together for simplicity. Phosphorylation levels of (F) AMPK Thr172, (G) ACC Ser212, and (H) TBC1D1 Ser231 were measured in lysates by western blotting (n = 10–12). Representative blots of these are given in (I), total proteins are given in Figure S3B. Data are given as means + SEM. WT and AMPKγ3 KO are indicated with white and red bars, respectively. One-way ANOVA (A) and two-way ANOVA (B–H) were used to compare treatment groups with vehicle and within genotypes, respectively. A: ***p < 0.001 for differences compared to vehicle. B: **p < 0.01, ***p < 0.001 for differences compared to vehicle and #p < 0.01 for differences compared to 20 µM treatment. C–H: *p < 0.05, **p < 0.01, ***p < 0.001 for differences compared to vehicle, #p < 0.05, ##p < 0.01, ###p < 0.001 for differences compared to 991 and $$p < 0.01, $$$p < 0.001 for differences compared to AICAR. A.U., Arbitrary Units. . (For interpretation of the references to colour in this figure legend, the reader is referred to the Web version of this article.)

WT muscle, while all interventions led to a significant increase in the muscle from AMPKγ3 KO mice (Figure 5H–I).

3.6. In vivo treatment with PF739 increases AMPKγ1 complex-associated activity

To investigate the whole-body transferability of the *ex vivo* studies, we tested the effect of *in vivo* treatment with PF739 on blood glucose levels, AMPK-complex-specific activity, and AMPK downstream regulation in muscle of HFD fed mice. Blood glucose levels were significantly higher in vehicle-treated mice. This might reflect a minor stress response owing to the handling of the animals. Nevertheless, blood glucose levels were lower in PF739-dosed mice compared to predosing levels and vehicle level 1 h after treatment (Figure 6A). AMPKα2β2γ3 activity in *m. gastrocnemius* did not increase in response to PF739 treatment. In contrast, the activation of AMPKγ1-complexes was increased by more than 2-fold, following PF739 dosing (Figure 6B). The phosphorylation of ACC was more than 3-fold higher in *m. gastrocnemius* than that of PF739-treated mice (Figure 6C).

4. DISCUSSION

Blood glucose-lowering pharmacological interventions are highly relevant, given the increase in prevalence of metabolic diseases worldwide. For more than two decades, it has been known that AMPK activation in skeletal muscle is sufficient to increase muscle glucose uptake [8]. Since then, a direct and safe way of pharmacologically targeting this kinase for blood glucose-lowering effects in humans has been striven for. Recently, it was revealed that ADaM-site binding small molecule pan activators of AMPK are capable of lowering blood glucose levels in diabetic rodent models through AMPK in skeletal muscle [16,17,24–26]. Unfortunately, nonskeletal muscle AMPK is also activated leading to unwanted side effects [17]. In this study, the mechanisms by which ADaM-site-binding AMPK activators increase glucose uptake in skeletal muscle were investigated. The study aimed to provide mechanistic insight that can lead to even better and more specific drug designs in the future.

We have previously shown that PF739 increases glucose uptake in glycolytic skeletal muscle [16]. We show here that combining two different ADaM-site activators (PF739 and 991) with AICAR potentiates the effect on glucose uptake in skeletal muscle *ex vivo*. These data indicate that ADaM-site activators and activators targeting the AMP-binding sites of the CBS domains increase glucose uptake by separate mechanisms. The mechanisms by which co-incubation causes potentiated AMPK complex activation are still unresolved. In a study in C2C12 muscle cells, it has been found that co-incubation of the ADaM-site binding compound A769662 and AICAR leads to a synergistic increase in the phosphorylation of AMPKα Thr172. This was ascribed to be partly due to conformational changes of AMPK since the compounds bind at two separate regions of AMPK, which increases the protection of AMPK from protein phosphatases [30]. Here, we show that the phosphorylation of AMPK Thr172 is indeed potentiated when co-stimulating muscle with PF739/991 and AICAR. In further support of this, maximal doses of the ADaM-site- and CBS-domain-binding compounds lead to a potentiated activation of AMPKα2β2γ3 and AMPKγ1-complexes, which may also indicate decreased accessibility of protein phosphatases towards AMPKα Thr172. However, further studies are needed to clarify the direct role of phosphatases in this regulation. Previously, additive effects on muscle glucose uptake and AMPK activation by co-incubation with 991 and AICAR have been reported [26]. However, since only submaximal doses were applied, an interpretation of the mechanisms involved was difficult. Importantly, in this study, for all used compounds or their combinations, the increase in glucose uptake observed in WT muscle was entirely ablated in AMPKα1α2-deficient muscle. Thus, the separate mechanisms by which the two compounds increase glucose uptake are fully AMPK-dependent and the co-incubation does not trigger any AMPK-independent effects on glucose uptake.

The effect of AICAR on glucose uptake in skeletal muscle is dependent on the AMPKα2β2γ3 complex [10,18,19] which is highly activated by AICAR treatment. The ability of AICAR to increase AMPKγ1-complex activity was present after 40 min of stimulation but absent after 60 min. Such time-dependency has not been exhibited in the skeletal muscle, whereas it has previously been reported in hepato- and adipocytes [31]. The mechanism underlying this attenuation is still unresolved. Nevertheless, our data strongly support that AMPKα2β2γ3 activation is necessary for AICAR-induced glucose uptake in skeletal muscle. As reasoned above, this data suggest that ADaM-site activators and AICAR increase glucose uptake by separate mechanisms. To seek genetic evidence for such a notion, EDL muscle of the AMPKγ3 KO mouse model was studied *ex vivo*. Remarkably, the effect of the ADaM-site activators on glucose uptake persisted in AMPKγ3-deficient muscle, whereas AICAR-stimulated glucose uptake was lost. These findings support that PF739- and 991-induced glucose uptake occur independently of the AMPKα2β2γ3 complex. The small molecule AMPK activator SC4 has been found to increase glucose uptake in muscle by an AMPKβ2-complex dependent mechanism [24].

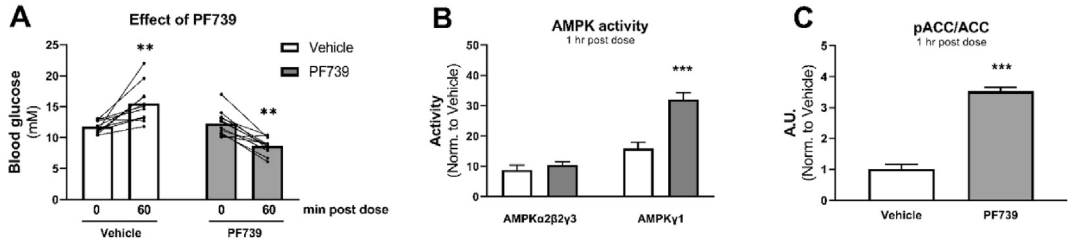

Figure 6: *In vivo treatment with PF739 lowers blood glucose and increases AMPKγ1 activity in skeletal muscle from diet-induced obese mice.* HFD fed mice were given a subcutaneous dose of either vehicle or PF739 (100 mg/kg) (n = 11–12). (A) Blood glucose levels were measured before and 1 h after treatment. (B) One hour after treatment the mice were anesthetized and muscles were harvested. *In vitro* complex-specific activity of AMPKα2β2γ3 and AMPKγ1-complexes was measured after sequential immunoprecipitation from *m. gastrocnemius* lysate in the order AMPKγ3, AMPKα2, and AMPKα1. The two latter are added together for simplicity. (C) Phosphorylation level of ACC Ser212 was measured in *m. gastrocnemius*. The paired individual data are indicated with dots and a connective line in (A). Data are given as means + SEM in (B–C). Vehicle and PF739 treatment are indicated with white and grey bars, respectively. A two-way ANOVA with RM was used in (A) to compare the effect of time and treatment. An unpaired students t-test was used in (B–C) to compare the effect of treatments. In (A) $^{**}p < 0.01$ indicates difference within treatment group and In (B–C) $^{***}p < 0.001$ indicates differences between vehicle and PF739 treatment. A.U., Arbitrary Units.

The structure of SC4 is slightly different from that of PF739 and 991, but SC4 also binds to the ADaM-site. If the AMPKβ2-selectivity holds true for all ADaM-site-binding compounds that increase muscle glucose uptake, then our data combined with that of Ngoei and colleagues [24], point toward the AMPKα2β2γ1 complex as a mediator of the glucose uptake as observed in response to ADaM-site-binding AMPK activators in general.

When ADaM-site activators are administered systemically to diabetic rodent models, blood glucose levels are lowered in a skeletal muscle AMPK-dependent manner [16,17]. Importantly, we show here that the AMPKγ1-complex activity is increased more than 2-fold, while the activity of AMPKα2β2γ3 is unchanged in muscle from mice treated with PF739 *in vivo*. In isolated muscles, the activation of AMPKγ1 was modest and did not reach statistical significance (PF739) or tended to be significant (991) in the muscles of both WT and AMPKγ3 KO. The reasons for these modest effects are unclear, especially since 991 has previously been demonstrated to increase AMPKγ1 activity [26]. Nevertheless, since AMPKγ2 has not been detected in skeletal muscle [4], we interpret our *in vivo* data to support the notion that treatment with ADaM-site activators uses a skeletal muscle AMPKγ1-dependent mechanism to increase glucose uptake and that this mechanism appears viable for effective treatment *in vivo.* It would be interesting to challenge this hypothesis in a muscle-specific AMPKγ1 KO model. To our knowledge, such a model has not yet been generated.

The reason why different modes of action exist for CBS-domain-binding compounds and ADaM-site activators to regulate glucose uptake is not known. It is tempting to consider that the difference might stem from the difference in the protein structure of the AMPKγ-isoforms i.e., the length of the N-terminal extension [32]. In a recent cell-based study, it was described that the level of activation induced by 991 was dependent on the γ-subunit expression [33]. Thus, it can be speculated that ADaM-site activators can only cause relevant levels of AMPK activation of certain AMPK complexes due to the structural differences of the AMPKγ-subunit proteins. Simultaneously, the CBS domains that are shared among the three AMPKγ proteins, are not equally sensitive to nucleotides [33—35]. This difference might affect the overall propensity of the different complexes to undergo necessary regulation by the ADaM-site activators to effectively regulate glucose transport. AMPKγ1 has been demonstrated to be highly nucleotide-sensitive, which may indicate that at physiological AMP levels, only AMPKγ1-complexes are primed for ADaM-site activators to be efficacious [34,35]. Lastly, evidence from cells also support the notion that different subcellular pools of AMPK are activated hierarchically under different conditions [36]. It is a reasonable explanation that our observations stem from the compounds activating different subcellular pools of AMPK, and that these are dominated by AMPKγ1 and AMPKγ3 for PF739/991 and AICAR, respectively. Thus, it could be speculated that the pools of AMPKγ1 activated by PF739 and AICAR are different and only the pool activated by PF739 regulates glucose transport. However, evidence of such subcellular pools in skeletal muscle tissue has to be established.

The lack of AICAR responsiveness that is often, but not always, reported in Sol muscle [10,13,37,38], has been linked to a very low or undetectable expression of AMPKγ3 protein [5]. However, it is difficult to understand why an ADaM-site binding activator such as PF739 that regulates glucose uptake through an AMPKγ3-independent mechanism, does not increase glucose uptake in Sol muscle, where AMPKγ1 protein is also highly expressed. In speculation, such discrepancy in pharmacologically-induced glucose uptake could be related to differences in glucose transport machinery between glycolytic (e.g. EDL) and oxidative (e.g. Sol) muscles, rather than differences at the level of AMPK. One example of such discrepancy is the AMPK-downstream target TBC1D1, the expression of which differs markedly between glycolytic and oxidative rodent muscles [39].

Collectively, our data suggest that several AMPK-heterotrimeric complexes in skeletal muscle are viable targets for glucose lowering pharmacological interventions. To date, the research field has focused mostly on AMPKγ3 in the skeletal muscle. The reasons for this partly relate to the vast amount of studies based on AICAR as a pharmacological research tool, and partly because of the tissue-specific expression of AMPKγ3, which makes AMPKγ3-drug targeting interventions muscle-specific, and thereby, less likely to cause major unwanted and deleterious side effects. However, with our findings in mind, an efficacious intervention does not need to be AMPKγ3-specific, provided it minimizes putative adverse effects of AMPK activation in nonmuscle tissues through other mechanisms. It has previously been demonstrated that 991 potently activates AMPKγ2-complexes *in vitro* [33], and furthermore, *in vivo* administration of an ADaM-site activator has been reported to lead to glycogen accumulation in cardiac muscle where AMPKγ2 is highly expressed [17]. These findings underline that skeletal muscle-specific targeting is of high importance for a future drug to be beneficial on a whole-body level. However, if an ADaM-site activator could be designed to target the muscle fiber only, the data provided here indicate that a glucose lowering effect through AMPKγ1-complexes would be just as effective as an AMPKγ3-specific activator. When this study was in the final stage of editing for submission, Rhein and colleagues verified the findings presented here in a similar approach, using similar experimental settings, but including different compounds and transgenic mouse models [40].

5. LIMITATIONS OF THIS STUDY

The AMPKγ3 KO mice used for the present study were backcrossed to a C57BL/6J background and bred as homozygotes for two generations. Thus, the reader should bear in mind the potential but minor risk of genetic drift in the cohorts. Pilot studies in mice of the inbred C57BL/6J strain revealed effect sizes equivalent to what is reported here. Furthermore, our data align with those of Rhein et al. [40] using a different AMPKγ3 model. Thus, although theoretically possible, there is no evidence to support that genetic drift has influenced our study or data interpretation.

6. CONCLUSION

We conclude that ADaM-site small molecule pan-AMPK activators regulate glucose uptake independently of AMPKγ3 in skeletal muscle. Furthermore, we conclude that ADaM-site activators and the prodrug AICAR increase glucose uptake through parallel mechanisms and this likely explains the potentiating effect observed on glucose uptake when these drugs are used in combination. We also observed compound potentiation of AMPKα2β2γ3 activation, though the nature behind this remains unresolved. Although we do not provide direct evidence for the

involvement of the AMPKγ1-complexes for ADaM-site-regulated glucose uptake, our data do suggest that stimulation of skeletal muscle glucose uptake can occur through different AMPK complexes.

FUNDING

This work was supported by grants from Pfizer Inc. and by grants given to JFPW: Danish Council for Independent Research (FSS: 6110-00498B).
This work was supported by a research grant to Rasmus Kjøbsted from the Danish Diabetes Academy, which is funded by the Novo Nordisk Foundation (NNF17SA0031406).
None of the funding bodies have had an influence on the conceptualization of the manuscript.

CONTRIBUTIONS

N.O.J., R.K., C.K.P., and J.F.P.W conceived and designed the research. N.O.J., R.K., M.R.L., J.B.B., N.R.A.,and B.A. performed the experiments. N.O.J. analyzed the data and drafted the manuscript. R.K. and J.F.P.W. contributed to manuscript drafting. R.M. and C.K.P. provided the PF739 compound and founder mice for the development of AMPKγ3 KO mice. D.C. provided the 991 compound. All authors contributed to data interpretation and discussion along with editing and revising of the manuscript. Furthermore, all authors read and approved the final version of the manuscript. J.F.P.W. is the guarantor of the work and had full access to all the data in the study and takes responsibility for the integrity of the data and the data analysis accuracy.

ACKNOWLEDGMENTS

The authors acknowledge the technical support given by Betina Bolmgren (Department of Nutrition, Exercise, and Sports, Faculty of Science, University of Copenhagen). Furthermore, the authors thank Prof. O. Göransson (Lund University, Sweden) and Prof. G. Hardie (University of Dundee, Scotland) for their kind gift of primary antibodies.
We thank Benoit Viollet and Marc Foretz (Inserm, France) for the donor AMPKα1α2-double-floxed mice.
Data from this study have previously been exhibited as poster presentations at two separate international conferences: AMPK — from Mechanisms to New Therapies (2018, Niagara-on-the-Lake, Canada) and Cell Exercise Metabolism conference (2019, Sitges, Spain).

CONFLICT OF INTEREST

Russell Miller and Bina Albuerquerque are currently employed at Pfizer Inc. (MA, USA).
Christian K. Pehmøller was employed at Pfizer Inc. (MA, USA) at the time of experiments.

APPENDIX A. SUPPLEMENTARY DATA

Supplementary data to this article can be found online at https://doi.org/10.1016/j.molmet.2021.101259.

REFERENCES

[1] Hardie, D.G., 2007. AMP-activated/SNF1 protein kinases: conserved guardians of cellular energy. Nature Reviews Molecular Cell Biology 8(10):774—785. https://doi.org/10.1038/nrm2249.
[2] Ross, F.A., MacKintosh, C., Hardie, D.G., 2016. AMP-activated protein kinase: a cellular energy sensor that comes in 12 flavours. FEBS Journal 283(16): 2987—3001. https://doi.org/10.1111/febs.13698.
[3] Wojtaszewski, J.F.P., Birk, J.B., Frøsig, C., Holten, M., Pilegaard, H., Dela, F., 2005. 5′AMP activated protein kinase expression in human skeletal muscle: effects of strength training and type 2 diabetes. The Journal of Physiology 564(2):563—573. https://doi.org/10.1113/jphysiol.2005.082669.
[4] Treebak, J.T., Birk, J.B., Hansen, B.F., Olsen, G.S., Wojtaszewski, J.F.P., 2009. A-769662 activates AMPK beta1-containing complexes but induces glucose uptake through a PI3-kinase-dependent pathway in mouse skeletal muscle. American Journal of Physiology - Cell Physiology 297(4):C1041—C1052. https://doi.org/10.1152/ajpcell.00051.2009.
[5] Mahlapuu, M., Johansson, C., Lindgren, K., Hjalm, G., Barnes, B.R., Krook, A., et al., 2004. Expression profiling of the gamma-subunit isoforms of AMP-activated protein kinase suggests a major role for gamma3 in white skeletal muscle. American Journal of Physiology. Endocrinology and Metabolism 286(2):E194—E200. https://doi.org/10.1152/ajpendo.00147.2003.
[6] Birk, J.B., Wojtaszewski, J.F.P., 2006. Predominant α2/β2/γ3 AMPK activation during exercise in human skeletal muscle. The Journal of Physiology 577(3):1021—1032. https://doi.org/10.1113/jphysiol.2006.120972.
[7] Kristensen, D.E., Albers, P.H., Prats, C., Baba, O., Birk, J.B., Wojtaszewski, J.F.P., 2015. Human muscle fibre type-specific regulation of AMPK and downstream targets by exercise. The Journal of Physiology 593(8): 2053—2069. https://doi.org/10.1113/jphysiol.2014.283267.
[8] Merrill, G.F., Kurth, E.J., Hardie, D.G., Winder, W.W., 1997. AICA riboside increases AMP-activated protein kinase, fatty acid oxidation, and glucose uptake in rat muscle. American Journal of Physiology 273(6 Pt 1):E1107—E1112. https://doi.org/10.1152/ajpendo.1997.273.6.E1107.
[9] Hayashi, T., Hirshman, M.F., Kurth, E.J., Winder, W.W., Goodyear, L.J., 1998. Evidence for 5' AMP-activated protein kinase mediation of the effect of muscle contraction on glucose transport. Diabetes 47(8):1369—1373. https://doi.org/10.2337/diabetes.47.8.1369.
[10] Jørgensen, S.B., Viollet, B., Andreelli, F., Frøsig, C., Birk, J.B., Schjerling, P., et al., 2004. Knockout of the α2 but not α1, 5′-AMP-activated protein kinase isoform abolishes 5-Aminoimidazole-4-carboxamide-1-β-4-ribofuranoside- but not contraction-induced glucose uptake in skeletal muscle. Journal of Biological Chemistry 279(2):1070—1079. https://doi.org/10.1074/jbc.M306205200.
[11] Hingst, J.R., Kjøbsted, R., Birk, J.B., Jørgensen, N.O., Larsen, M.R., Kido, K., et al., 2020. Inducible deletion of skeletal muscle AMPK a reveals that AMPK is required for nucleotide balance but dispensable for muscle glucose uptake and fat oxidation during exercise. Molecular Metabolism 40(June):101028. https://doi.org/10.1016/j.molmet.2020.101028.
[12] Fisher, J.S., Gao, J., Han, D.H., Holloszy, J.O., Nolte, L.A., 2002. Activation of AMP kinase enhances sensitivity of muscle glucose transport to insulin. American Journal of Physiology. Endocrinology and Metabolism 282(1):E18—E23. https://doi.org/10.1152/ajpendo.00477.2004.
[13] Kjøbsted, R., Treebak, J.T., Fentz, J., Lantier, L., Viollet, B., Birk, J.B., et al., 2015. Prior AICAR stimulation increases insulin sensitivity in mouse skeletal muscle in an AMPK-dependent manner. Diabetes 64(6):2042—2055. https://doi.org/10.2337/db14-1402.
[14] Kjøbsted, R., Munk-Hansen, N., Birk, J.B., Foretz, M., Viollet, B., Björnholm, M., et al., 2017. Enhanced muscle insulin sensitivity after contraction/exercise is mediated by AMPK. Diabetes 66(3):598—612. https://doi.org/10.2337/db16-0530.
[15] Kjøbsted, R., Pedersen, A.J.T., Hingst, J.R., Sabaratnam, R., Birk, J.B., Kristensen, J.M., et al., 2016. Intact regulation of the AMPK signaling network in response to exercise and insulin in skeletal muscle of male patients with type 2 diabetes: illumination of AMPK activation in recovery from exercise. Diabetes 65(5):1219—1230. https://doi.org/10.2337/db15-1034.
[16] Cokorinos, E.C., Delmore, J., Reyes, A.R., Albuquerque, B., Kjøbsted, R., Jørgensen, N.O., et al., 2017. Activation of skeletal muscle AMPK promotes

glucose disposal and glucose lowering in non-human primates and mice. Cell Metabolism 25(5):1147—1159. https://doi.org/10.1016/j.cmet.2017.04.010 e10.

[17] Myers, R.W., Guan, H.-P., Ehrhart, J., Petrov, A., Prahalada, S., Tozzo, E., et al., 2017. Systemic pan-AMPK activator MK-8722 improves glucose homeostasis but induces cardiac hypertrophy. Science 357(6350):507—511. https://doi.org/10.1126/science.aah5582.

[18] Steinberg, G.R., O'Neill, H.M., Dzamko, N.L., Galic, S., Naim, T., Koopman, R., et al., 2010. Whole body deletion of AMP-activated protein kinase β2 reduces muscle AMPK activity and exercise capacity. Journal of Biological Chemistry 285(48):37198—37209. https://doi.org/10.1074/jbc.M110.102434.

[19] Barnes, B.R., Marklund, S., Steiler, T.L., Walter, M., Hjalm, G., Amarger, V., et al., 2004. The 5 '-AMP-activated protein kinase gamma 3 isoform has a key role in carbohydrate and lipid metabolism in glycolytic skeletal muscle. Journal of Biological Chemistry 279(37):38441—38447. https://doi.org/10.1074/jbc.M405533200.

[20] Dixon, R., Gourzis, J., McDermott, D., Fujitaki, J., Dewland, P., Gruber, H., 1991. AICA-riboside: safety, tolerance, and pharmacokinetics of a novel adenosine-regulating agent. The Journal of Clinical Pharmacology 31(4):342—347. https://doi.org/10.1002/j.1552-4604.1991.tb03715.x.

[21] Calabrese, M.F., Rajamohan, F., Harris, M.S., Caspers, N.L., Magyar, R., Withka, J.M., et al., 2014. Structural basis for AMPK activation: natural and synthetic ligands regulate kinase activity from opposite Poles by different molecular mechanisms. Structure 22(8):1161—1172. https://doi.org/10.1016/j.str.2014.06.009.

[22] Pinkosky, S.L., Scott, J.W., Desjardins, E.M., Smith, B.K., Day, E.A., Ford, R.J., et al., 2020. Long-chain fatty acyl-CoA esters regulate metabolism via allosteric control of AMPK β1 isoforms. Nature Metabolism 2(9):873—881. https://doi.org/10.1038/s42255-020-0245-2.

[23] Cool, B., Zinker, B., Chiou, W., Kifle, L., Cao, N., Perham, M., et al., 2006. Identification and characterization of a small molecule AMPK activator that treats key components of type 2 diabetes and the metabolic syndrome (June). p. 403—16. https://doi.org/10.1016/j.cmet.2006.05.005.

[24] Ngoei, K.R.W., Langendorf, C.G., Ling, N.X.Y., Hoque, A., Varghese, S., Camerino, M.A., et al., 2018. Structural determinants for small-molecule activation of skeletal muscle AMPK α2β2γ1 by the glucose importagog SC4. Cell Chemical Biology 25(6):728—737. https://doi.org/10.1016/j.chembiol.2018.03.008.

[25] Lai, Y.-C., Kviklyte, S., Vertommen, D., Lantier, L., Foretz, M., Viollet, B., et al., 2014. A small-molecule benzimidazole derivative that potently activates AMPK to increase glucose transport in skeletal muscle: comparison with effects of contraction and other AMPK activators. Biochemical Journal 460(3):363—375. https://doi.org/10.1042/BJ20131673.

[26] Bultot, L., Jensen, T.E., Lai, Y.-C., Madsen, A.L.B., Collodet, C., Kviklyte, S., et al., 2016. Benzimidazole derivative small-molecule 991 enhances AMPK activity and glucose uptake induced by AICAR or contraction in skeletal muscle. American Journal of Physiology - Endocrinology And Metabolism 311(4):E706—E719. https://doi.org/10.1152/ajpendo.00237.2016.

[27] Lantier, L., Fentz, J., Mounier, R., Leclerc, J., Treebak, J.T., Pehmøller, C., et al., 2014. AMPK controls exercise endurance, mitochondrial oxidative capacity, and skeletal muscle integrity. Federation of American Societies for Experimental Biology Journal 28(7):3211—3224. https://doi.org/10.1096/fj.14-250449.

[28] Fentz, J., Kjøbsted, R., Kristensen, C.M., Hingst, J.R., Birk, J.B., Gudiksen, A., et al., 2015. AMPKα is essential for acute exercise-induced gene responses but not for exercise training-induced adaptations in mouse skeletal muscle, 00157 American Journal of Physiology - Endocrinology And Metabolism: Ajpendo(2015). https://doi.org/10.1152/ajpendo.00157.2015.

[29] Birk, J.B., Wojtaszewski, J.F.P., 2018. Kinase activity determination of specific AMPK complexes/heterotrimers in the skeletal muscle. AMPK. Methods in Molecular Biology. New York, NY: Humana Press. p. 215—28.

[30] Ducommun, S., Ford, R.J., Bultot, L., Deak, M., Bertrand, L., Kemp, B.E., et al., 2014. Enhanced activation of cellular AMPK by dual-small molecule treatment: AICAR and A769662. American Journal of Physiology. Endocrinology and Metabolism 306(6):E688—E696. https://doi.org/10.1152/ajpendo.00672.2013.

[31] Corton, J.M., Gillespie, J.G., Hawley, S.A., Hardie, D.G., 1995. 5-aminoimidazole-4-carboxamide ribonucleoside. A specific method for activating AMP-activated protein kinase in intact cells? European Journal of Biochemistry 229(2):558—565 https://doi.org/10.1111/j.1432-1033.1995.tb20498.x.

[32] Cheung, P.C., Salt, I.P., Davies, S.P., Hardie, D.G., Carling, D., 2000. Characterization of AMP-activated protein kinase gamma-subunit isoforms and their role in AMP binding. Biochemical Journal 346(Pt 3):659—669. https://doi.org/10.1042/0264-6021:3460659.

[33] Willows, R., Navaratnam, N., Lima, A., Read, J., Carling, D., 2017. Effect of different γ-subunit isoforms on the regulation of AMPK. Biochemical Journal 474(10):1741—1754. https://doi.org/10.1042/BCJ20170046.

[34] Ross, F.A., Jensen, T.E., Hardie, D.G., 2016. Differential regulation by AMP and ADP of AMPK complexes containing different γ subunit isoforms. Biochemical Journal 473(2):189—199. https://doi.org/10.1042/BJ20150910.

[35] Rajamohan, F., Reyes, A.R., Frisbie, R.K., Hoth, L.R., Sahasrabudhe, P., Magyar, R., et al., 2016. Probing the enzyme kinetics, allosteric modulation and activation of α1- and α2-subunit-containing AMP-activated protein kinase (AMPK) heterotrimeric complexes by pharmacological and physiological activators. Biochemical Journal 473(5):581—592. https://doi.org/10.1042/BJ20151051.

[36] Zong, Y., Zhang, C.-S., Li, M., Wang, W., Wang, Z., Hawley, S.A., et al., 2019. Hierarchical activation of compartmentalized pools of AMPK depends on severity of nutrient or energy stress. Cell Research 29(6):460—473. https://doi.org/10.1038/s41422-019-0163-6.

[37] Chadt, A., Immisch, A., Wendt, C. De., Springer, C., Zhou, Z., Stermann, T., et al., 2015. Deletion of both Rab-GTPase — activating proteins TBC1D1 and TBC1D4 in mice eliminates insulin- and AICAR-stimulated. Glucose Transport 64(March 2014):746—759. https://doi.org/10.2337/db14-0368.

[38] Stöckli, J., Meoli, C.C., Hoffman, N.J., Fazakerley, D.J., Pant, H., Cleasby, M.E., et al., 2015. The RabGAP TBC1D1 plays a central role in exercise-regulated glucose metabolism in skeletal muscle. Diabetes 64(6):1914—1922. https://doi.org/10.2337/db13-1489.

[39] Taylor, E.B., An, D., Kramer, H.F., Yu, H., Fujii, N.L., Roeckl, K.S.C., et al., 2008. Discovery of TBC1D1 as an insulin- , AICAR- , and contraction-stimulated signaling nexus in. Mouse Skeletal Muscle * 283(15):9787—9796. https://doi.org/10.1074/jbc.M708839200.

[40] Rhein, P., Desjardins, E.M., Rong, P., Ahwazi, D., Bonhoure, N., Stolte, J., et al., 2021. Compound- and fiber type-selective requirement of AMPKγ3 for insulin-independent glucose uptake in skeletal muscle. Molecular Metabolism, 101228. https://doi.org/10.1016/j.molmet.2021.101228.

